PNAS RESEARCH ARTICLE | NEUROSCIENCE OPEN ACCESS

Cx43 hemichannels contribute to astrocyte-mediated toxicity in sporadic and familial ALS

Akshata A. Almad[a,1], Arens Taga[a,1], Jessica Joseph[a,1], Sarah K. Gross[a], Connor Welsh[a], Aneesh Patankar[a], Jean-Philippe Richard[a], Khalil Rust[a], Aayush Pokharel[a], Caroline Plott[a], Mauricio Lillo[b], Raha Dastgheyb[a], Kevin Eggan[c], Norman Haughey[a], Jorge E. Contreras[b,d], and Nicholas J. Maragakis[a,2]

Edited by Anders Björklund, Lund University, Lund, Sweden; received May 4, 2021; accepted December 16, 2021

Connexin 43 (Cx43) gap junctions and hemichannels mediate astrocyte intercellular communication in the central nervous system under normal conditions and contribute to astrocyte-mediated neurotoxicity in amyotrophic lateral sclerosis (ALS). Here, we show that astrocyte-specific knockout of Cx43 in a mouse model of ALS slows disease progression both spatially and temporally, provides motor neuron (MN) protection, and improves survival. In addition, Cx43 expression is up-regulated in human postmortem tissue and cerebrospinal fluid from ALS patients. Using human induced pluripotent stem cell–derived astrocytes (hiPSC-A) from both familial and sporadic ALS, we establish that Cx43 is up-regulated and that Cx43-hemichannels are enriched at the astrocyte membrane. We also demonstrate that the pharmacological blockade of Cx43-hemichannels in ALS astrocytes using GAP 19, a mimetic peptide blocker, and tonabersat, a clinically tested small molecule, provides neuroprotection of hiPSC-MN and reduces ALS astrocyte-mediated neuronal hyperexcitability. Extending the in vitro application of tonabersat with chronic administration to SOD1^{G93A} mice results in MN protection with a reduction in reactive astrocytosis and microgliosis. Taking these data together, our studies identify Cx43 hemichannels as conduits of astrocyte-mediated disease progression and a pharmacological target for disease-modifying ALS therapies.

astrocyte | stem cells | connexin

Significance

Our results demonstrate that connexin 43 hemichannels are the conduits for amyotrophic lateral sclerosis (ALS) astrocyte-mediated motor neuron toxicity and disease spread, acting as a common mechanism that can target both familial ALS and sporadic ALS populations. Furthermore, our present work provides proof of principle that tonabersat, as a drug already studied in clinical trials for other indications, could serve as a potential ALS therapeutic.

Astrocytes form a highly coupled intercellular network in the central nervous system (CNS) through gap junctions (GJ) and hemichannels (HC) (1). GJ facilitate intercellular communication through the exchange of metabolites (2, 3), ions (4, 5), second messengers (6, 7), and microRNA (8). Each GJ is composed of two adjoining HC on the plasma membrane of adjacent cells and each HC is made of six connexin subunits arranged around a central pore (9). While connexins mostly form GJ, they can also exist as nonjunctional HC that open at the plasma membrane into the extracellular space. HC opening is dynamic and especially relevant as HC open upon cellular damage and under pathological conditions (10–12). Connexin 43 (Cx43) is the predominant connexin in astrocytes and the major contributor to astrocyte HC (11, 13–15). Some key roles of Cx43 include (16–19) homeostatic buffering, synchronization of astrocyte networks, metabolic support for neurons, and modulation of synaptic activity and plasticity.

In amyotrophic lateral sclerosis (ALS), astrocytes carrying disease-specific mutations contribute to disease progression after onset and exacerbate motor neuron (MN) toxicity (20–22). ALS astrocyte-mediated neurotoxicity has also been demonstrated in vitro and in vivo using both murine (22, 23) and human ALS astrocytes (24–27). Recent studies suggest cytokines can infuence specific astrocyte profiles that render astrocytes to be proinflammatory causing toxicity across several neurodegenerative diseases (28).

Altered Cx43 expression and function, including GJ coupling and HC activity, occurs in a number of neurological diseases (10, 11). In ALS, we have previously reported Cx43 is increased in the lumbar spinal cord of the ALS mouse model expressing mutant superoxide dismutase (SOD1^{G93A}) (29), and demonstrated using an in vitro mouse model that blocking Cx43 in SOD1^{G93A} astrocytes is neuroprotective.

This work now addresses a central role for astrocytes in ALS, their involvement in disease progression, and whether Cx43 HC are a common mechanism contributing to MN death in both familial (FALS) and sporadic ALS (SALS) patients. To that end, we utilize an in vivo conditional Cx43 knockout (KO) mouse model to demonstrate that astrocyte Cx43 contributes to the temporal progression of disease. Using human brain and spinal cord tissues, as well as cerebrospinal fluid (CSF) from ALS patients, we demonstrate that Cx43 expression is enhanced in ALS and has some correlation with

Author affiliations: [a]Department of Neurology, The Johns Hopkins University School of Medicine, Baltimore, MD 21205; [b]Department of Pharmacology, Physiology, & Neuroscience, New Jersey Medical School, Rutgers University, Newark, NJ 07101; [c]Department of Stem Cell and Regenerative Biology, Harvard University, Cambridge, MA 02138; and [d]Department of Physiology and Membrane Biology, School of Medicine, University of California, Davis, CA 95616

Author contributions: A.A.A., A.T., J.J., J.E.C., and N.J.M. designed research; A.A.A., A.T., J.J., S.K.G., C.W., A. Patankar, J.-P.R., K.R., A. Pokharel, C.P., M.L., R.D., N.H., J.E.C., and N.J.M. performed research; A.A.A., A.T., J.J., S.K.G., C.W., A. Patankar, J.-P.R., K.R., A. Pokharel, C.P., M.L., R.D., K.E., N.H., J.E.C., and N.J.M. analyzed data; and A.A.A., A.T., J.J., S.K.G., J.-P.R., C.P., M.L., R.D., K.E., N.H., J.E.C., and N.J.M. wrote the paper.

The authors declare a competing interest. K.E. is a founder of and consultant for Q-state Biosciences, Quralis, and Enclear therapies. N.J.M. has filed US Patent Application #16868764 titled "Neuroprotective Compounds for ALS."

This article is a PNAS Direct Submission.

[1]A.A.A., A.T., and J.J. contributed equally to this manuscript.

[2]To whom correspondence may be addressed. Email: nmaragak@jhmi.edu.

This article contains supporting information online at http://www.pnas.org/lookup/suppl/doi:10.1073/pnas.2107391119/-/DCSupplemental.

Published March 21, 2022.

the rapidity of disease progression in tissues. Our fully humanized, spinal cord-specific platform of SALS and FALS human-induced pluripotent stem cell astrocyte (hiPSC-A) and MN (hiPSC-MN) cocultures enable us to investigate whether blocking Cx43 HC in hiPSC-A using a small molecule has functional relevance in providing neuroprotection to a broad ALS patient population. Finally, we translate these in vitro findings to in vivo treatment of SOD1^{G93A} mice, demonstrating the potential of Cx43 HC blockade as a strategy for neuroprotection.

Results

Astrocyte-Specific Deletion of Cx43 in SOD1^{G93A} Mice Slows Temporal and Anatomical Disease Progression. We have shown (29) that Cx43 expression increases during the symptomatic and end stages of disease in the SOD1^{G93A} mouse model of ALS and that astrocytes from these mice display functional increases in Cx43-mediated GJ and HC activity in vitro. To assess the role of astrocyte Cx43 in vivo in the context of ALS, we crossed the SOD1^{G93A} mouse with a Cx43fl/fl:GFAP-Cre mice to specifically delete Cx43 in astrocytes (Fig. 1). Examination of the ventral horn of the lumbar spinal cord, where loss of MN is particularly evident, shows an increase in Cx43 expression in SOD1^{G93A} mice, as expected (29). However, Cx43fl/fl:SOD1^{G93A}:GFAP-Cre (SOD1^{G93A}:Cx43 KO) mice have a near complete loss of Cx43 expression in the ventral horn, as demonstrated by immunofluorescence (Fig. 1 *A* and *B*). This decrease in Cx43 expression is accompanied by a reduction in GFAP expression in the SOD1^{G93A}:Cx43 KO mice (Fig. 1 *A* and *B*). In addition, we verified that while Cx43 expression is typically elevated at the symptomatic and end stages in the SOD1^{G93A} model, it remains knocked out through end stage (Fig. 1*C*). The KO of Cx43 in astrocytes of SOD1^{G93A} mice was anatomically consistent across different segments of spinal cord (Fig. 1*C*).

To assess whether the loss of astrocyte Cx43 affects MN survival and disease progression, we performed pathological and motor behavioral studies, specifically grip strength analysis, on SOD1^{G93A}:Cx43 KO mice during the course of disease. We did not observe any differences in the timing of hindlimb disease onset in SOD1^{G93A}:Cx43 KO mice (Fig. 1*D*). However, the SOD1^{G93A}:Cx43 KO mice displayed prolonged survival compared to their littermate control SOD1^{G93A} mice (Fig. 1*E*). While the disease onset started at the same time, as reflected in motor function using hindlimb grip strength (Fig. 1*F*), the forelimb grip strength of SOD1^{G93A}:Cx43 KO was significantly maintained compared to the decline observed in the control SOD1^{G93A} mice (Fig. 1*F*). We examined whether this sustained forelimb function, indicative of slower disease progression in the SOD1^{G93A}:Cx43 KO mice, was due to preservation of cervical spinal cord MNs. We observed a significant protection of cervical MN (but not lumbar MN) in the SOD1^{G93A}:Cx43 KO spinal cord compared to control SOD1^{G93A} (Fig. 1*G*).

While we previously did not detect any substantial change in Cx30 expression (29), the other major astrocyte connexin in SOD1^{G93A} mice, SOD1^{G93A}:Cx43 KO mice show a modest up-regulation of Cx30 in the gray matter, potentially as a compensatory effect from loss of Cx43 (*SI Appendix*, Fig. S1*A*). No changes were observed in microglial reactivity measured by Iba-1 immunostaining, and the astrocyte-specific glutamate transporter, GLT-1, was also unchanged in the lumbar spinal cord (*SI Appendix*, Fig. S1*A*). We also validated that the transgene expression of mutant human SOD1 levels were similar in SOD1^{G93A}:Cx43 KO mice and the control litter mate SOD1^{G93A} mice (*SI Appendix*, Fig. S1*B*). As MN protection was observed in the cervical cord, we examined both astrogliosis (GFAP) and microgliosis (Iba1) and a significant decrease was noted in the SOD1^{G93A}:Cx43 KO mice compared to their littermate control SOD1^{G93A} mice (*SI Appendix*, Fig. S1*C*).

We further confirmed that the neuroprotection seen in vivo was recapitulated in an in vitro SOD1^{G93A} astrocyte/WT MN cocultures (29). We first validated that not only do SOD1^{G93A} astrocytes exhibit an increase in Cx43 expression, but that the SOD1^{G93A}:Cx43 KO astrocytes lack Cx43 expression, as expected (*SI Appendix*, Fig. S1 *E* and *F*). Upon coculturing these astrocytes with Hb9GFP MNs, we demonstrate that SOD1^{G93A} astrocytes induce MN toxicity, and this effect is rescued in cocultures with SOD1^{G93A}:Cx43 KO astrocytes resulting in neuroprotection (*SI Appendix*, Fig. S1*G*). These data show that deletion of Cx43 (both GJs and HCs) in general has a beneficial protective effect in vivo in the SOD1 ^{G93A} mice.

Previous work (28, 30) suggests that activated astrocytes can have either a proinflammatory or "A1" profile that is neurotoxic or an antiinflammatory "A2" profile that confers neuroprotection. However, our work suggests that the mechanism of toxicity to MNs from SOD1^{G93A} astrocytes and of neuroprotection from SOD1^{G93A}:Cx43 KO astrocytes is disparate from the shift in astrocyte "activation state" (*SI Appendix*, Fig. S1*H*) (28, 30).

Elevated Cx43 Is Disproportionately Incorporated into HCs in SOD1^{G93A} Mouse Astrocytes. Having established the role of Cx43 in astrocyte-mediated MN loss and disease progression in a murine ALS model, we wanted to determine the specific contribution of Cx43 GJ vs. HC to these phenomena. As we observed significant neuroprotection with Cx43 HC blocker in vitro (29), we hypothesized that Cx43 is primarily present as HC on the astrocyte membrane. We used a previously described (31) biotin pulldown assay to specifically target Cx43 HC, which have exposed lysine residues and can bind to biotin in monolayer cultures, thereby allowing us to determine what proportion of Cx43 is present as HC (*SI Appendix*, Fig. S2 *A–C*). Interestingly, we observed that 9.6 ± 2.1% of Cx43 incorporate as HCs in WT astrocytes, whereas 32.8 ± 4.7% of Cx43 form HCs in SOD1^{G93A} astrocytes (*SI Appendix*, Fig. S2*D*). While there is an overall increase in Cx43 levels in SOD1^{G93A} (*SI Appendix*, Fig. S2*E*), the absolute levels of Cx43 HC were specifically elevated in diseased cells compared to WT astrocytes (*SI Appendix*, Fig. S2*F*). These data suggest that there is more total Cx43 protein present on the surface of SOD1^{G93A} astrocytes than in WT, and that this amount represents an abnormal shift in the percentage of total Cx43 expression to HC formation. As a negative control, we used the SOD1^{G93A}:Cx43 KO astrocytes and found that the Cx43 KO cells do not have a measurable quantity of either total Cx43 or Cx43 in HC form compared to WT and SOD1^{G93A} astrocytes (*SI Appendix*, Fig. S2*G*).

Cx43 Expression Is Increased in Human ALS Postmortem Tissue and CSF. Having demonstrated the distribution of Cx43 and its relevance to MN loss in murine ALS models, we then examined this biology in ALS patients. Previously, we demonstrated an increase in Cx43 expression in a cohort of ALS patient motor cortex and spinal cord (29). Here, we inquired if there is a correlation between Cx43 expression and the temporal course of disease. We examined an expanded cohort of SALS motor cortex and cervical spinal cord (*SI Appendix*, Table S1) and observed an increase in Cx43 and GFAP transcript levels in the motor cortex of post mortem SALS patients (*SI*

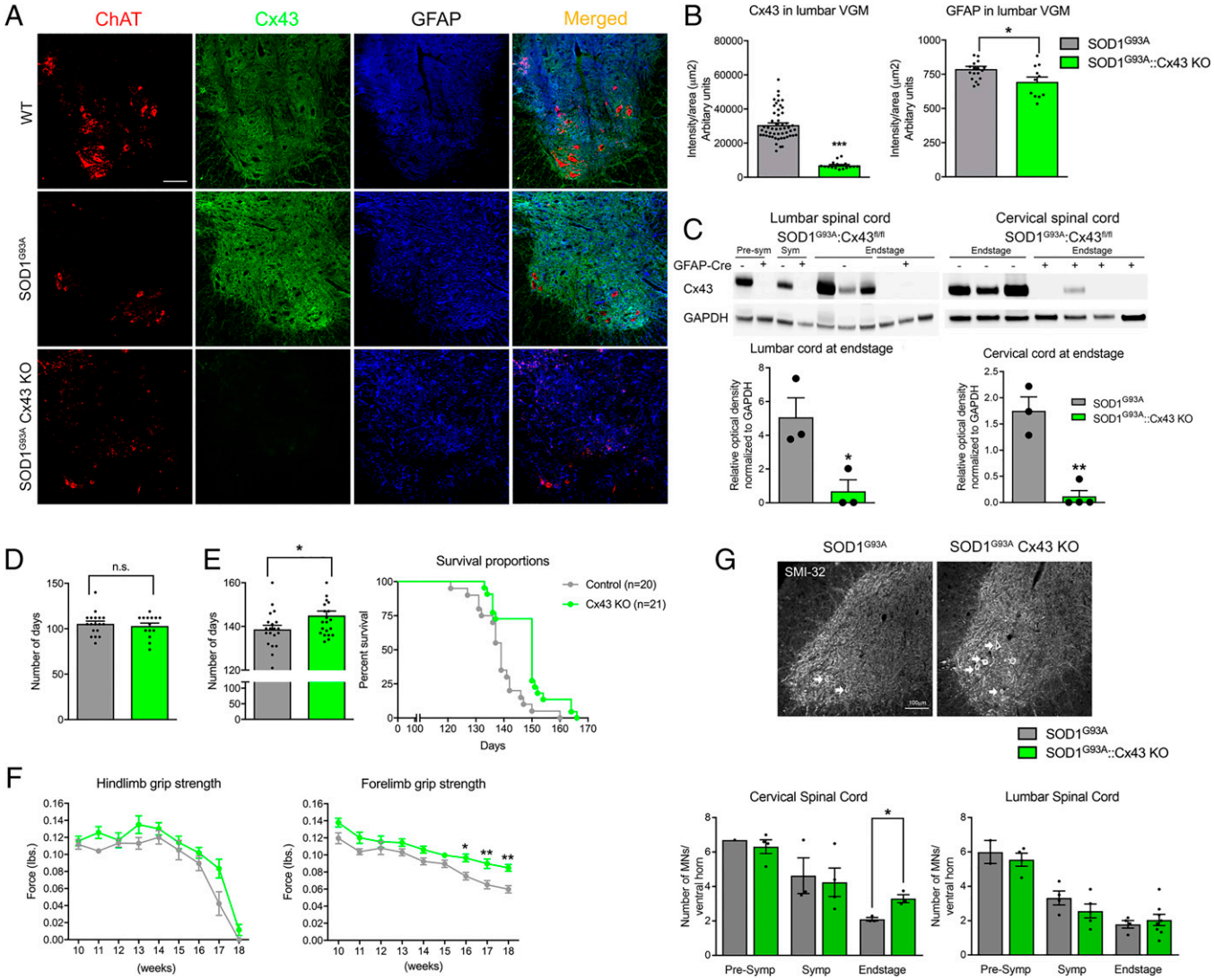

Fig. 1. Astrocyte-specific deletion of Cx43 improves survival and slows caudal rostral progression in SOD1^{G93A} mice. (*A* and *B*) Cx43$^{fl/fl}$ mice were bred with a GFAP-Cre driver line, which were further crossed with SOD1^{G93A} mice to generate a triple transgenic mouse (SOD1^{G93A}:Cx43 KO). The MNs located in the ventral spinal cord are labeled with ChAT immunostain. The immunohistochemical staining confirms the lack of Cx43 staining in the lumbar spinal cord of the SOD1^{G93A}:Cx43 KO mice compared to WT and control SOD1^{G93A} mice. A reduction in astrogliosis was observed based on GFAP immunoreactivity in the SOD1^{G93A}:Cx43 KO mice compared to SOD1^{G93A} mice. *$P < 0.05$, ***$P < 0.001$, $n = 4$ animals per group, and at least three sections per animal. (Scale bar, 100 μm.) (*C*) Immunoblotting confirmed the deletion of Cx43 in SOD1^{G93A}:Cx43$^{fl/fl}$: GFAP-Cre^{+} mice in the lumbar spinal cord at presymptomatic, symptomatic, and end stage of disease. Cx43 is also absent in cervical spinal cord of the SOD1^{G93A}:Cx43$^{fl/fl}$:GFAP-Cre^{+} ($n = 3$ to 5 animals per group) **$P < 0.01$. (*D*) SOD1^{G93A}:Cx43 KO mice and littermate SOD1^{G93A} mice show similar time of disease onset. (*E*) SOD1^{G93A}:Cx43 KO mice survived significantly longer (145 ± 2.1, $n = 21$) compared to SOD1^{G93A} mice (138.7 ± 1.9, $n = 20$), also depicted in the Kaplan–Meier survival curve, *$P < 0.05$. (*F*) Motor function was tested using grip-strength analysis and SOD1^{G93A}:Cx43 KO mice maintained significantly higher forelimb grip strength compared to SOD1^{G93A} mice with no overall change in hindlimb grip strength. *$P < 0.05$, **$P < 0.01$. ($n = 16$ to 20). (*G*) No differences in MN survival were noted at presymptomatic and symptomatic stages of the disease in the cervical and lumbar spinal cord. However, a significant preservation of MNs was observed at end stage in the cervical spinal cord of SOD1^{G93A}:Cx43 KO mice ($n = 3$ per group) compared to SOD1^{G93A} mice but not in the lumbar cord. ($n = 4$ to 8 per group), *$P < 0.05$. Data are represented as mean ± SEM.

Appendix, Fig. S3 *A* and *B*). This increase in Cx43 transcript parallels protein expression levels in ALS-affected brain regions, such as the motor cortex and cervical spinal cord, when compared to controls. Given the heterogeneity in disease progression, we inquired whether there is a correlation with Cx43 expression. ALS patients with rapidly progressing disease (i.e., deceased within 2 y after onset) (32, 33) display higher Cx43 protein levels in motor cortex compared to both control and patients with a more typical ALS disease progression (i.e., deceased between 2 and 5 y after onset) (32, 33) (*SI Appendix*, Fig. S3*C*). This correlation between increased Cx43 levels and ALS disease progression also holds true for cervical spinal cord samples (*SI Appendix*, Fig. S3*D*). By using ELISA, we demonstrated that Cx43 protein is detected in vivo in the CSF from control and ALS patients. As observed in postmortem tissue, Cx43 protein level was significantly elevated in the CSF samples obtained from ALS patients (*SI Appendix*, Fig. S3*E*).

Astrocyte Cx43 HC Expression and Function Is Increased in hiPSC-A from both FALS and SALS Patients. To assess if Cx43-mediated effects in ALS extend beyond SOD1 mutations, we examined Cx43 expression in cells obtained from a cohort of patients with both SALS and FALS (*SI Appendix*, Table S2) and differentiated them into hiPSC-A using a spinal cord patterning protocol (34) (*SI Appendix*, Fig. S4 *A–D*). Consistent with our previous findings, similar degrees of astrocyte differentiation occur between control, FALS and SALS hiPSC-A, as indicated by astrocyte markers (*SI Appendix*, Fig. S4 *E–H*) (34).

A consistent and significant increase in Cx43 expression was observed in hiPSC-A from SALS patients (Fig. 2*A*). In addition, we investigated Cx43 changes in FALS hiPSC-A specifically from three different slowly progressing $SOD1^{D90A}$ and from three unrelated fast-progressing $SOD1^{A4V}$ patients (Fig. 2*B*). While $SOD1^{D90A}$ samples display a trend for an increase in Cx43 expression, the fast-progressing $SOD1^{A4V}$ hiPSC-A show a significant increase in Cx43 expression compared to control hiPSC-A (Fig. 2*B*). As hiPSC-A are differentiated in the absence of neurons (*SI Appendix*, Fig. S4), any change in Cx43 occurs independently of neuronal input (cell autonomous) and not as a secondary effect of neuron-dependent astrocyte "activation." Confirming this, we observed that the expression of Cx43 in FALS and SALS hiPSC-A remains significantly elevated in hiPSC-A/MN cocultures as well (*SI Appendix*, Fig. S5).

Intriguingly, Cx43 levels in hiPSC-A exhibit a correlation with ALS disease progression similar to ALS postmortem samples. While Cx43 expression is increased in $SOD1^{D90A}$ cases (who have a relatively slower temporal course), Cx43 levels are further significantly higher in patients with $SOD1^{A4V}$ mutation (who exhibit a faster disease progression) compared to control patients (35) (Fig. 2*B*). Similar to the murine in vitro studies above, we determined the specific contribution of Cx43 HC to the amount of total Cx43 using ALS hiPSC-A. We used the biotinylation assay for FALS hiPSC-A (Fig. 2 *C*–*G*), as described for *SI Appendix*, Fig. S2, and observed that both control and the FALS hiPSC-A expressed similar proportional amounts of Cx43 as HC (Fig. 2*D*). Therefore, when quantified, the percentages of Cx43 present as HC were not significantly different (Fig. 2*E*). However, FALS astrocytes had higher absolute levels of Cx43 expression (Fig. 2 *F* and *G*). We extended our analysis to the absolute amounts of Cx43 HC between pulldowns from control and SALS patient lines, and noted that all ALS hiPSC-A lines had higher absolute amounts of Cx43 HC present on their membranes (Fig. 2*H*).

The release of ATP through the Cx43 HC opening has been reported in other neurodegenerative diseases (36) as a measure for Cx43 HC activity. Hence, we tested the opening of Cx43 HC by measuring ATP release via a luciferase assay in the supernatants of FALS and SALS hiPSC-A. Endogenous ATP in this instance acts as a functional marker for HC opening. At baseline, both FALS and SALS hiPSC-A had higher concentrations of ATP in their supernatant compared to hiPSC-A from controls. Upon treatment with Gap19, a Cx43 HC-specific mimetic peptide blocker (37), control ATP supernatant levels were unchanged but ATP levels in both the FALS and SALS hiPSC-A supernatants, were reduced to control ranges (Fig. 2 *I* and *J*). This suggests that, at baseline, ALS hiPSC-A have increased HC permeability to ATP that can be pharmacologically blocked.

Blocking Cx43 HC in Human ALS iPSC-A Mitigates MN Toxicity. Given the opportunity to examine the genetic and phenotypic heterogeneity of ALS using hiPSC-A, we cocultured hiPSC-A (Fig. 3*A*) from control and two unrelated FALS ($SOD1^{A4V}$) patients with hiPSC-MN from controls. We found that FALS hiPSC-A induced toxicity in human iPSC-MN ($ChAT^+$), including a subset of $Isl1^+$ MNs, and that blocking Cx43 HC with Gap19 provided significant neuroprotection (Fig. 3 *A*–*K*). Similarly, we employed an identical coculture paradigm to examine whether hiPSC-A from SALS patients would be toxic to control hiPSC-MN (Fig. 3*A*). We observed a similar level of hiPSC-MN toxicity compared to the $SOD1^{A4V}$ hiPSC-A and also demonstrated neuroprotection via HC blockade using Gap19 (Fig. 3 *A*–*K*).

In order to test Cx43 HC-specific neurotoxicity, we hypothesized that ALS hiPSC-A toxicity was conferred by a factor released into the medium, as might be expected for connexin HC. To this end, we performed a hiPSC-A/MN coculture study where hiPSC-A were grown on a transwell insert above and control hiPSC-MN on the base of the well, with both cell groups grown in the same media (Fig. 3*L*). We cocultured FALS and SALS hiPSC-A lines with hiPSC-MN derived from control patients, and observed a significant reduction in hiPSC-MN survival as defined by ChAT and Isl1 immunostaining, similar to the direct coculture paradigm (Fig. 3 *L*–*V*). We also treated the transwell cocultures with Gap19, which resulted in significant neuroprotection from both FALS hiPSC-A, as well as SALS hiPSC-A–induced toxicity (Fig. 3 *L*–*V*). These data suggest that astrocyte-mediated toxicity from these ALS lines is propagated mainly through Cx43 HC and further demonstrate the neuroprotective effect of Gap19 in FALS and SALS astrocytes. To rule out the effect of Gap19 directly on neurons, we confirmed that the addition of Gap19 to hiPSC-MN cultures alone did not affect MN survival and thus neuroprotection is specifically mediated by astrocytes (*SI Appendix*, Fig. S6*A*).

While much of ALS in vitro biology is focused on MN loss, there is in vivo evidence (38–40) that other neuronal populations are affected by neurodegeneration. We utilized our hiPSC-based platform to examine whether non-MN degeneration in ALS is astrocyte and specifically Cx43 HC-mediated. Our data utilizing human ALS hiPSC-A/MN cocultures show that ALS astrocytes from both SALS and FALS patients also induce toxicity to $TUJ1^+/ChAT^-$ neurons. This effect was partially rescued by the addition of the Cx43 HC blocker Gap19 (*SI Appendix*, Fig. S6*B*). We established, by using the transwell system and Gap19, as described above, that this ALS astrocyte-mediated neurotoxicity was related to a factor released through Cx43 HC (*SI Appendix*, Fig. S6*C*). Furthermore, we have reproduced our findings on astrocyte and Cx43 HC-mediated hiPSC-A neurotoxicity toward MN and non-MN populations using a different control hiPSC-neuronal line (CS25) (*SI Appendix*, Fig. S7).

Gene Correction of $SOD1^{A4V}$ in hiPSC-A Results in Reduced Cx43 Expression and MN Protection. To examine if correction of the $SOD1^{A4V}$ mutation attenuated Cx43 expression, we used a previously (41) characterized ALS $SOD1^{A4V}$ hiPSC line and its gene-corrected isogenic control line (*SI Appendix*, Fig. S8*A*). As expected, Cx43 protein levels were higher in the ALS $SOD1^{A4V}$ hiPSC-A compared to control astrocytes, while the corresponding gene-corrected $SOD1^{A4V}$ line showed a partial normalization of Cx43 expression (*SI Appendix*, Fig. S8*B*). These data indicate that increases in Cx43 expression are a common feature of both SALS and FALS patients. Interestingly, when the $SOD1^{A4V}$ mutation was corrected using zinc finger endonuclease, the resulting isogenic line displayed residual neurotoxicity on hiPSC-MN in a coculture paradigm (*SI Appendix*, Fig. S8 *C*–*M*). This neurotoxicity could be further rescued by Cx43 HC blockade with Gap19 (*SI Appendix*, Fig. S8*C*). This was confirmed in the transwell platform as well (*SI Appendix*, Fig. S8 *N*–*X*), where the correction of the $SOD1^{A4V}$ mutation in the FALS hiPSC-A line conferred partial neuroprotection, with the residual neurotoxicity being further rescued by Cx43 HC blockade with Gap19.

The Cx43 HC Blocker Tonabersat Decreases Astrocyte-Mediated hiPSC-MN Death and Hyperexcitability in a Dose-Dependent Manner. Our findings from rodent models and human ALS samples suggest that Cx43 HC may provide an appropriate target for ALS therapeutics. Tonabersat (SB-

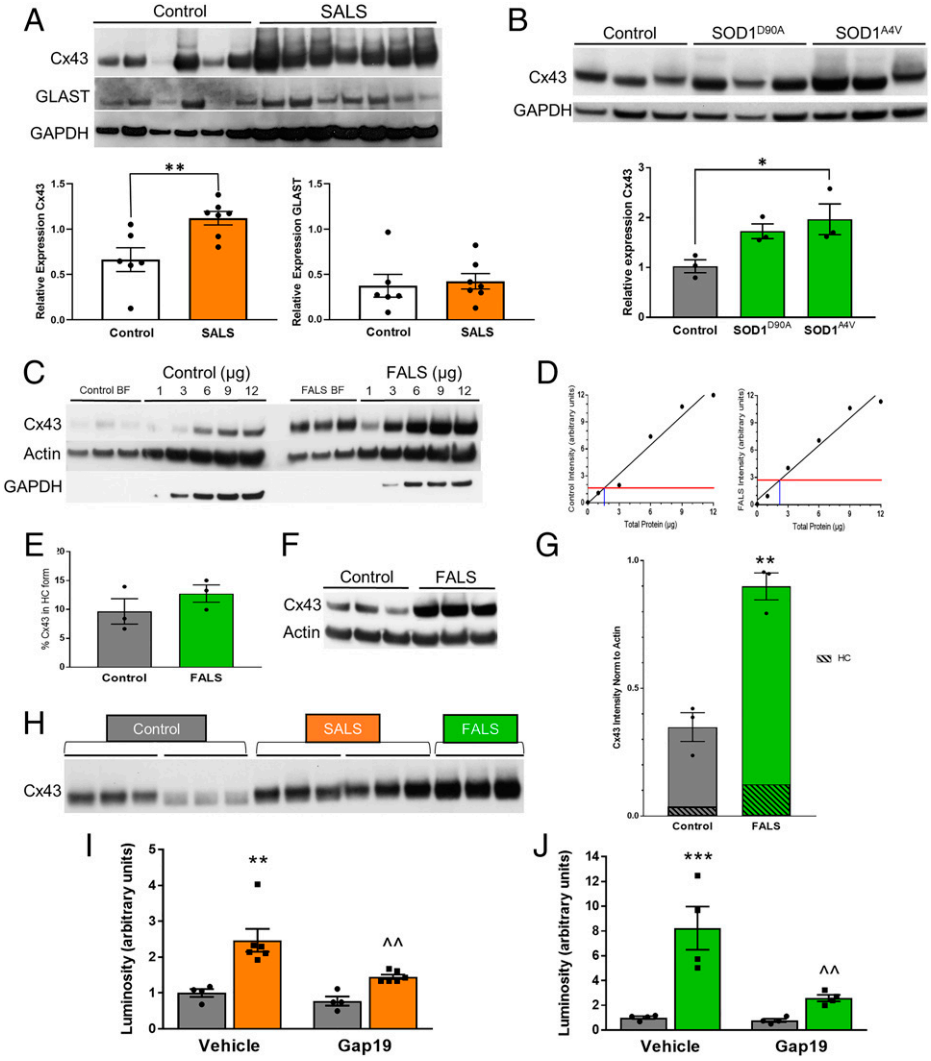

Fig. 2. Human ALS iPSC-A have increased Cx43 HC levels associated with increased cell permeability, which can be blocked by Gap19. (*A*) Western blots of total protein collected from various hiPSC-A control and SALS lines were compared for the expression of Cx43 and GLAST (EAAT1), a glial-specific membrane protein. Quantification shows sporadic Cx43 expression is significantly higher, while no difference was found in the expression of GLAST. Control lines from left to right: GO018, CS25, JH082, CIPS, JH003, GM01582. SALS lines from left to right: JH013, JH036, JH053, JH029, JH017 JH058, JH040 (**$P < 0.01$, *t* test, $n = 6$ to 7 per condition). (*B*) Western blots stained for Cx43 in hiPSC-A from control and familial lines shows that in $SOD1^{A4V}$ patients, Cx43 expression is significantly higher. Control lines from left to right CIPS, GM01582, JH082. $SOD1^{D90A}$-lines left to right: GO017, GO004, GO028. $SOD1^{A4V}$ lines left to right: GO013, GO002, GO007 (*$P < 0.05$, one-way ANOVA, $n = 3$ per condition). (*C*) Control (CIPS) and FALS hiPSC-A (GO013) in vitro lines were subjected to biotin pulldown. Subsequent biotin fractions and total protein were immunoblotted for Cx43, with actin and GAPDH as housekeeping genes. (*D*) Linear quantification against the total protein standards have R^2 values of 0.97 and 0.96. (*E*) There is no statistically significant shift in the percent of Cx43 as HC between ALS and control hiPSC-A. (*F*) Western blot of total protein for hiPSC-A control and FALS lines. (*G*) FALS has significantly more Cx43 than control (**$P < 0.01$, $n = 3$). When percentages from 4E are mapped against total protein, FALS has more Cx43 in HC than control. (*H*) Western blot of two lines from control (CIPS, GM01582) and SALS (JH058, JH040), and one line of FALS (GO013) stained for Cx43 from the biotin fraction in vitro. Each bar represents one line tested in triplicate. (*I*) ATP levels detected in the supernatants of control and sporadic hiPSC-A show significantly higher amounts in SALS hiPSC-A compared to controls. Treatment with Gap19 significantly reduces supernatant ATP in sporadic astrocytes (two-way ANOVA, **$P <$ 0.01, ^^$P < 0.01$, $n = 4$ to 6). (*J*) Supernatant ATP of FALS hiPSC-A is significantly higher than control. Gap19 reduces supernatant ATP of FALS hiPSC-A compared to vehicle treatment (two-way ANOVA, ***$P <$ 0.001, ^^$P < 0.01$, $n = 4$). Data are represented as mean ± SEM.

220453) was selected for its translational potential in human clinical trials (42, 43). It specifically blocked Cx43 HC at low concentrations (1 to 10 µM), but not the astrocytic Cx30 HC, as demonstrated in a heterologous expression system (44) (*SI Appendix*, Fig. S9).

To examine the potential of tonabersat in preventing hiPSC-A and Cx43 HC-mediated neurotoxicity, we cocultured control hiPSC-MN with either control hiPSC-A, FALS hiPSC-A, or SALS hiPSC-A. We utilized direct coculture (Fig. 4 *A–K*) and transwell (Fig. 4 *L–V*) paradigms as described above, and found that tonabersat protects hiPSC-MN from ALS astrocyte-mediated death in a dose-dependent manner in both systems. At 1 and 10 µM, tonabersat blocks Cx43 HC and rescues $ChAT^+$ MNs, including a subpopulation of $Isl1^+$ MN. At a higher concentration of 100 µM, tonabersat was not neuroprotective, and likely reflects a long-term effect on reducing GJ trafficking instead of HC activity, as described previously (42) (Fig. 4 *A–K*). The neuroprotective effect of tonabersat was also seen in the transwell study (Fig. 4 *L–V*), suggesting that tonabersat's neuroprotection is HC-mediated and further confirming the importance of Cx43 HC in toxicity. We believe that the neuroprotective effects of tonabersat are specific to Cx43 HC on astrocytes, since the application of tonabersat to cultures of hiPSC-MN alone did not have any effect on hiPSC-MN survival (*SI Appendix*, Fig. S10*A*). Interestingly, we also observed that tonabersat was protective to non-MN populations ($ChAT^-$ and $Isl1^-$ neurons), similar to the results seen with Gap19 treatment (*SI Appendix*, Fig. S10 *B* and *C*).

In the CNS, tonabersat's actions may translate to an astrocyte-mediated reduction of neuronal excitability (45, 46), as suggested by in vivo studies showing tonabersat's inhibitory effects on cortical spreading depression (47, 48) and seizures (49, 50). We have previously used (34) multielectrode array (MEA) in a fully human iPSC-based platform to evaluate how astrocytes influence MN electrophysiology (*SI Appendix*, Fig. S11*A*), and here we employ that system to evaluate the electrophysiological actions of tonabersat in vitro. We first utilized control cocultures of hiPSC-A/MN on MEA plates to study how the pharmacological blockade of hiPSC-A Cx43 HC would affect hiPSC-MN electrophysiological activity. The addition of tonabersat (*SI Appendix*, Fig. S11*B*) at a concentration of 10 µM significantly reduced neuronal spiking and bursting activity within 5 min of application. The effect was dose-dependent, as a lower concentration of tonabersat (i.e., 1 µM) was less effective (*SI Appendix*, Fig. S11*B*). These actions parallel those of the Cx43 HC-specific blocker Gap19 (*SI Appendix*, Fig. S11*C*), confirming our previous observations that Cx43 HC influences neuronal firing (34). To ensure that these effects

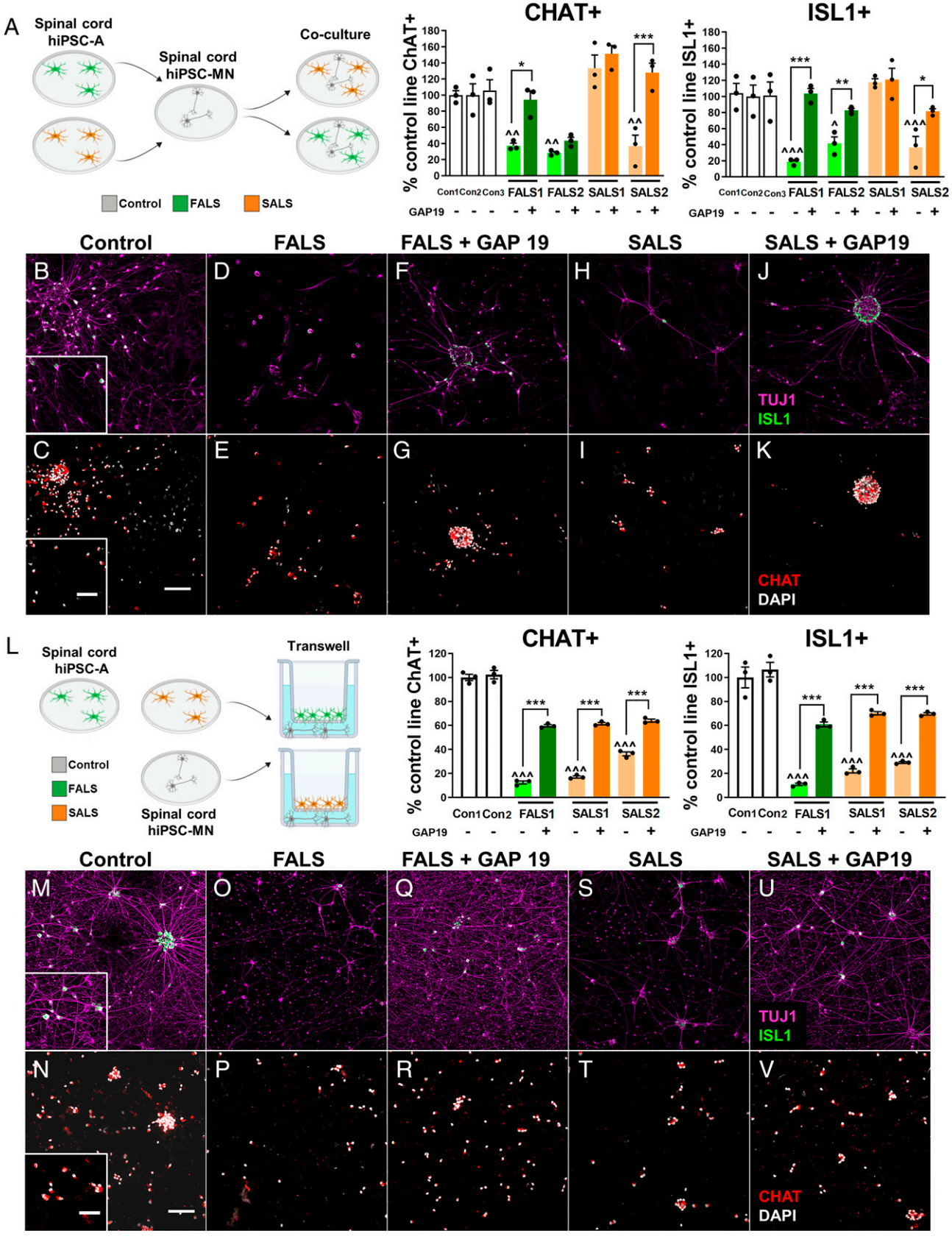

Fig. 3. Human iPSC-MN toxicity is mediated by Cx43 HC from FALS as well as SALS hiPSC-A. (*A–K*) MNs derived from control hiPSC were plated with hiPSC-A from either control, SALS, or FALS ($SOD1^{A4V}$) patients. The number of hiPSC-MN ($ChAT^+$ and $Isl\text{-}1^+$) plated on FALS and SALS hiPSC-A decreased over a period of 14 d compared to MN plated with control hiPSC-A. Cocultures containing ALS hiPSC-A treated with Gap19 show an increase in hiPSC-MN survival. (*L–V*) The coculture of hiPSC-A/-MN in a transwell system allowed neurons and astrocytes to share the same medium, preventing direct cell contact. FALS ($SOD1^{A4V}$) and SALS hiPSC-A shows $ChAT^+$ and $Isl\text{-}1^+$ hiPSC-MN toxicity rescued by Gap19. Con1 = CIPS, Con2 = JH082, Con3 = GM01582, FALS1 = GO013, FALS2 = GO002, SALS1 = JH040, SALS2 = JH058 (n = 3 coverslips per condition). Significant comparisons (one-way ANOVA) between untreated control and ALS cocultures are marked with "^"; significant effects of Gap19 on cocultures containing ALS astrocytes are marked with "*". *$P < 0.05$ and ^$P < 0.05$; **$P < 0.01$ and ^^$P < 0.01$; ** $P < 0.001$ and ^^^$P < 0.001$. (Scale bars, 50 μm main panel; *Inset* is 20 μm.) Data are represented as mean ± SEM.

were astrocyte-mediated, we tested tonabersat on hiPSC-MN alone in culture and did not observe any change in neuronal electrophysiological activity (*SI Appendix*, Fig. S11*D*).

We then evaluated these electrophysiological findings in the context of ALS (Fig. 5) and cocultured control and ALS hiPSC-A with control hiPSC-MN and recorded them longitudinally for 2 wk. A transient increase in neuronal spiking and bursting activity was observed in the cocultures of SALS and FALS hiPSC-A when compared to control cocultures (Fig. 5*A*). This occurs early during the 2-wk recording period (significant at day in vitro [DIV] 6 of coculture), followed by a depression of electrophysiological activity (DIV 14 of coculture). Acute treatment with tonabersat significantly reduced this transient ALS astrocyte-mediated hyperexcitability (Fig. 5*B*), leading to spiking and bursting activity that are comparable to untreated control cocultures.

We then evaluated if there is a temporal correlation between astrocyte-mediated neuronal hyperexcitability and Cx43 HC-mediated neurotoxicity in ALS. To address this, we used the coculture paradigm with ALS and control hiPSC-A/MN cocultures with a shorter treatment course with tonabersat (Fig. 5*C*). We observed that early application of 10 μM tonabersat (i.e., from day 5 to day 8 of coculture) confers neuroprotection of hiPSC-MN in coculture with ALS hiPSC-A, which corresponds to the time period of neuronal hyperexcitability based on MEA recordings. However, when the cocultures are treated with tonabersat at a later time-point (from day 11 to day 14 of coculture), when neuronal hypoactivity occurs in ALS hiPSC-A cocultures (based on MEA recordings), there is no neuroprotection. Examination of MN survival at day 11 of coculture confirmed that the early window of neuroprotection is critical as most MN death has occurred prior to that time, thus not allowing for neuroprotection from the later addition of tonabersat (*SI Appendix*, Fig. S12). Therefore, there appears to be a critical early window of time during which tonabersat provides this temporal neuroprotection, which is seen not only in MNs, but also in ChAT$^-$ neurons (Fig. 5*C*).

Tonabersat Provides In Vivo Neuroprotection in SOD1^{G93A} Mice. To test whether the neuroprotective effects of tonabersat on ALS iPSC-MN translated in vivo, we treated a cohort of SOD1^{G93A} mice starting at a presymptomatic stage (40 d of age) with daily administration of tonabersat at 10 mg/kg (*SI Appendix*, Fig. 13*A*). As predicted, Cx43 expression was increased in the ventral horn of SOD1^{G93A} spinal cord in vehicle-treated mice but, interestingly, we did not see an altered expression of Cx43 in SOD1^{G93A} mice treated with tonabersat (*SI Appendix*, Fig. S13 *B–E*). Tonabersat treatment in SOD1^{G93A} mice significantly reduced both astrogliosis, measured with GFAP (*SI Appendix*, Fig. S13 *B–E*), as well as microgliosis (Iba-1) (*SI Appendix*, Fig. S13 *B* and *C*). While the neuroprotective effect of tonabersat was not yet evident at the early symptomatic stages for SOD1^{G93A} mice (*SI Appendix*, Fig. S13*F*), a significant preservation of MN in the cervical spinal cord (*SI Appendix*, Fig. S13*G*), and to a lesser degree the lumbar spinal cord, was noted in tonabersat-treated SOD1^{G93A} mice compared to vehicle-treated SOD1^{G93A} mice. A trend toward preservation of forelimb grip strength was noted without an effect on survival. To test whether tonabersat had any toxicity when delivered chronically from 40 d of age, WT mice were treated with tonabersat and vehicle. We did not appreciate any toxic effect on MN number, behavior, or survival in WT mice (*SI Appendix*, Fig. S13 *G–I*).

To examine whether treatment after symptom onset could provide neuroprotection, another cohort of SOD1^{G93A} mice was treated with tonabersat after disease onset beginning at 100 d of age (*SI Appendix*, Fig. S14*A*). As with the mice whose treatment began at 40 d of age, neuroprotection was again seen in the cervical spinal cord (*SI Appendix*, Fig. S14*B*). Trends toward maintenance in forelimb grip strength were again observed in both the 100 d of age-treated cohorts (*SI Appendix*, Fig. S14*C*). Together, these in vivo data suggest that effects of blocking Cx43 HC-mediated MN toxicity is most evident following disease onset.

Discussion

Cx43 is the predominant connexin in astrocytes (11, 13–15, 51) and is unique as it is the only astrocyte connexin that can be incorporated into HCs as well as GJs. Changes in Cx43 expression are reported in neurodegenerative disorders, primarily as an up-regulation of the protein (29, 52–55), although less is known about the degree to which these increases are incorporated specifically into the HC, GJ, or both (56).

In ALS, few studies have shown increased total Cx43 in lumbar spinal cord of SOD1^{G93A} mice, although the implications for the increases in total Cx43 protein were not examined (57–59). In our previous study (29), we observed an increase in expression of Cx43 in this ALS mouse model and in SOD1^{G93A} astrocytes occurring cell autonomously, in the absence of neurons or neuronal death (29).

Astrocytes have been implicated in ALS progression after disease onset (21). In order to investigate astrocyte Cx43-specific contributions in vivo and in disease progression, we generated a triple transgenic SOD1^{G93A} mouse with Cx43 KO in astrocytes using GFAP-Cre mice. While the disease onset was not affected by astrocyte-specific Cx43 KO, we observed sustained forelimb motor function and an overall increase in survival in this mouse model. These observations suggest that astrocyte Cx43 influences both the temporal course after onset and the anatomical progression of disease. The alteration of the temporal and anatomical progression following KO of astrocyte Cx43 and Cx30 has similarly been reported in a spinal cord injury model (60). Previous studies in Alzheimer's disease, however, have suggested that GJ coupling may be a mechanism for compensatory neuroprotection by buffering potentially toxic substances through the astrocyte network and away from at-risk neurons (61, 62). Therefore, it may be that the KO of Cx43, which affects both GJ and HC formation in our SOD1^{G93A}:Cx43 KO mice, may actually underestimate the potential neuroprotective effect of Cx43 HC loss alone. This would be consistent with our previous data in SOD1^{G93A} in vitro studies showing that pharmacologic blockade of Cx43 HC provided equivalent neuroprotection to the less specific pharmacological blockade of both Cx43 GJ and HC (29). Interestingly, we did not appreciate that SOD1^{G93A} astrocytes had a toxic "A1" profile nor did the KO of Cx43 in the SOD1^{G93A} astrocytes mirror what had previously been described as a neuroprotective "A2" profile (28). At least in this paradigm, our data would suggest that molecular phenotypes related to "activated" ALS astrocyte-mediated MN toxicity may be more complex among disease states.

Cx43 is incorporated into both GJs as well as HCs. Hence, we tested whether the increases in Cx43 observed in SOD1^{G93A} mice primarily affects Cx43 HC at the astrocyte membrane. Previous studies relied on pharmacologic blockade with peptide blockers to implicate Cx43 HC relevance in the context of disease (11, 29). By modifying a biotin pulldown method (31),

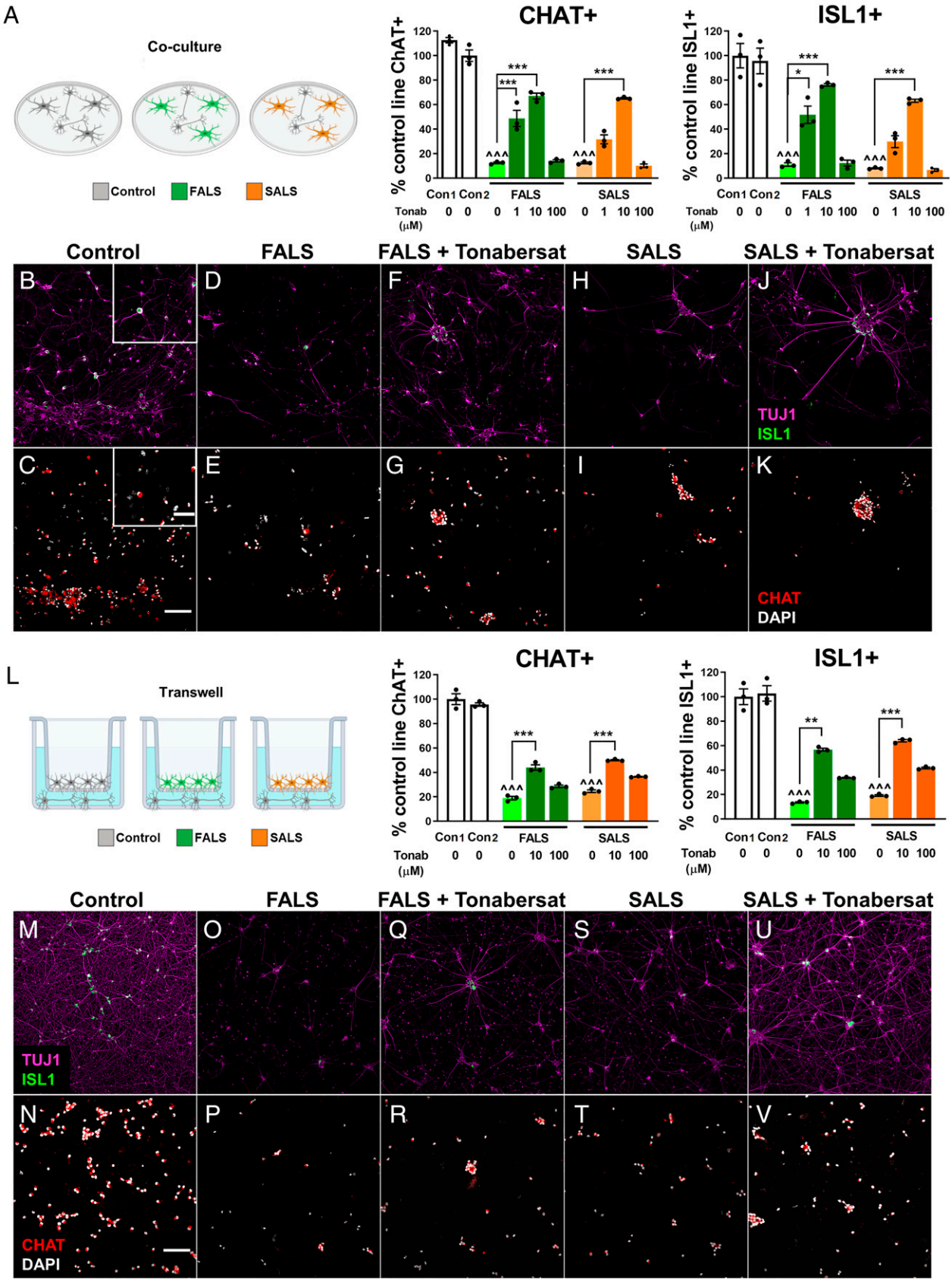

Fig. 4. The Cx43 HC blocker tonabersat provides dose-dependent neuroprotection to hiPSC-MN. (*A–K*) FALS and SALS hiPSC-A/MN cocultures immunostained for ChAT and Isl-1 show dose-dependent neuroprotection from tonabersat (1 μM, 10 μM, and 100 μM), after a 14-d incubation period. (*L–V*) Following transwell coculture of FALS and SALS hiPSC-A with hiPSC-MN, immunostaining for ChAT$^+$ MN and Isl1$^+$ MN confirms dose-dependent neuroprotection with tonabersat. Con1 = CIPS, Con2 = GM01582, FALS = GO013, SALS = JH058. Significant comparisons (one-way ANOVA) between untreated control and ALS cocultures are marked with "^"; significant effects of tonabersat on cocultures containing ALS astrocytes are marked with "*". *$P < 0.05$ and ^$P < 0.05$; **$P < 0.01$ and ^^$P < 0.01$; ***$P < 0.001$ or ^^^$P < 0.001$, $n = 3$ per condition. (Scale bars, 50 μm main panel; *Inset* is 20 μm.) Data are represented as mean ± SEM.

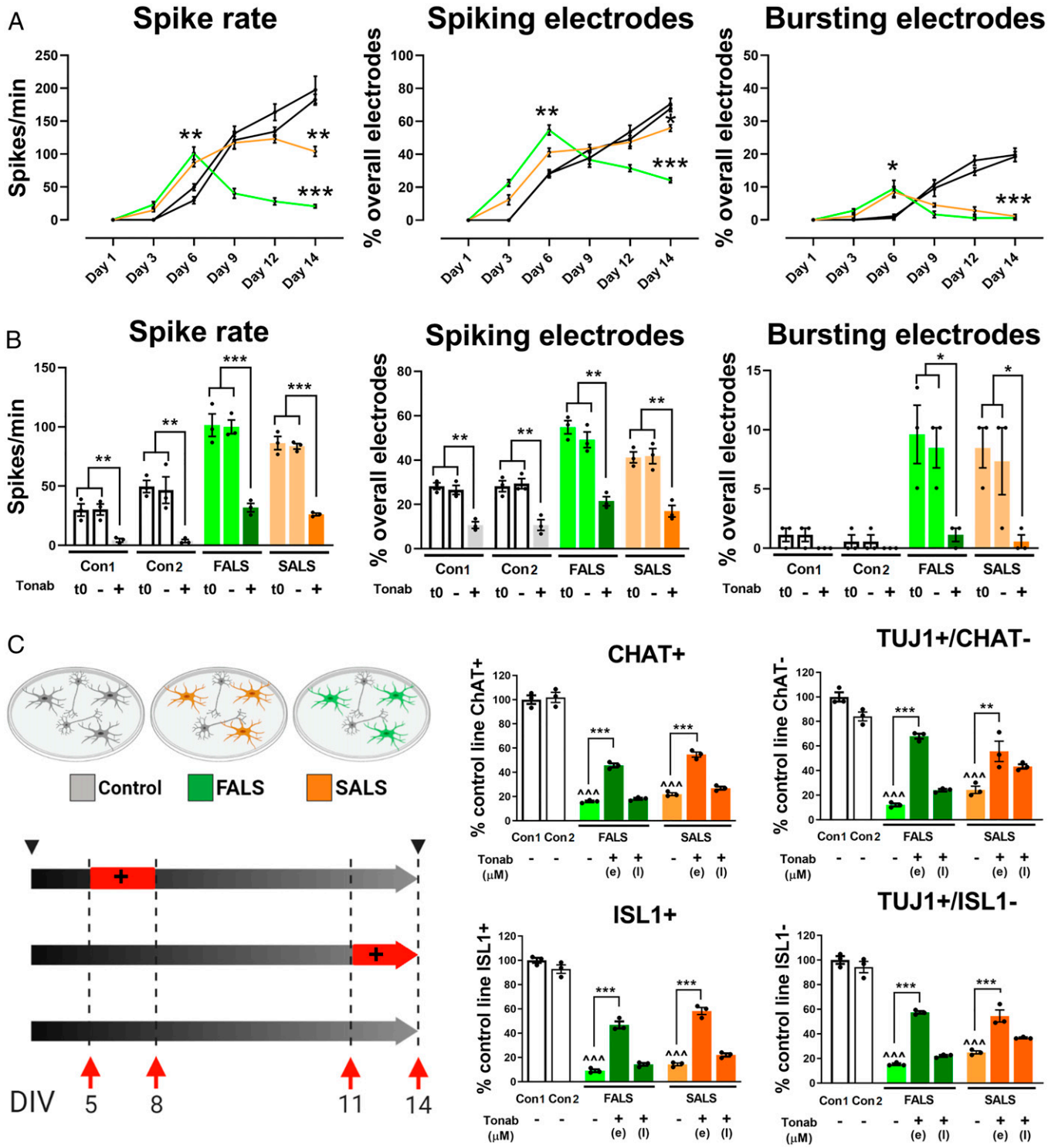

Fig. 5. MEA recordings from hiPSC-Astro/MN cultures demonstrate that tonabersat Cx43 HC-mediated effects on hiPSC-MN electrophysiology correlates with neuroprotection. (*A*) MEA recording of neuronal activity from cocultures between control hiPSC-MN and control or ALS hiPSC-A. The presence of SALS and FALS astrocytes when compared to control astrocytes determines early increases in spiking and bursting activity followed, at later time points, by reduced electrophysiological activity. Significant time-point comparisons (i.e., day 6 and 14 of coculture) between control and ALS conditions are marked with an asterisk (*) (black line = control, orange line = SALS, green line = FALS). (*B*) MEA activity within 5 min after the application of 10 μM tonabersat (+) on cocultures with control or ALS hiPSC-A compared to baseline (*t*0) and vehicle (−). MEA baseline activity at day 6 shown in *A*. Tonabersat shows significant inhibition (*) of neuronal spiking and bursting activity. (*C*) The effects of 10 μM tonabersat (+) on hiPSC-neuron survival in control and ALS cocultures was tested as outlined in the figure, but for a shorter time course of 3 d, either early (DIV 5 to 8, or "e") or late (DIV 11 to 14 or "l") during coculture. Significant neuroprotection was appreciated after early but not late exposure to tonabersat; evident for both MN (ChAT$^+$ and ISL1$^+$ cells) and non-MN cell types (TUJ1$^+$/ChAT$^-$, TUJ1$^+$/ISL1$^-$). Con1 = CIPS, Con2 = GM01582, FALS = GO013, SALS = JH058. Significant comparisons (one-way ANOVA) between untreated control and ALS cocultures are marked with (^), while significant effects of tonabersat on cocultures containing ALS astrocytes are marked with (*). *P < 0.05 and ^P < 0.05; **P < 0.01 and ^^P < 0.01; ***P < 0.001 and ^^^P < 0.001, n = 3 per condition. Data are represented as mean ± SEM.

we directly demonstrated increases in the total amount of Cx43 in its HC form. Interestingly, in the $SOD1^{G93A}$ mice, the actual proportion of Cx43 in HC was significantly higher than the percentage seen in WT. This provides evidence that the up-regulation of Cx43 may be the result of altered HC trafficking toward or from astrocytic membranes as well.

Human iPSC-A derived from FALS patients carrying SOD1 mutations as well as from SALS patients provide a unique in vitro tool to investigate astrocyte contributions to neurodegeneration. Importantly, we could begin to address whether both FALS and SALS populations have Cx43 HC-mediated neurotoxicity. Similar to the $SOD1^{G93A}$ mouse astrocytes, we noted that increases in Cx43 expression in our library of hiPSC-A lines from both FALS and SALS patients. A gene-corrected isogenic $SOD1^{A4V}$ hiPSC-A line resulted in a reduction in Cx43 expression. Our data are particularly notable as these ALS hiPSC-A have never been in coculture with MN and, therefore, the increases in Cx43 are not determined by neuronal signals, as we have previously (34) described in hiPSC-A/-MN cocultures, nor have they been exposed to neuronal cell death as occurs in vivo. Previous evidence has suggested that epigenetic profiles, including age- and disease-dependent signatures, may not be affected by the reprogramming process and, therefore, may constitute a residual "epigenetic memory" (63), as demonstrated by studies utilizing hiPSC-A for modeling FALS and SALS and other neurodegenerative disorders (64). While studying the potential mechanisms regulating Cx43 expression was beyond the aims of the present study, there is evidence suggesting that intrinsic changes in Cx43 expression in ALS hiPSC-A may arise from an altered metabolic state of reprogrammed astrocytes (65), changes in transcriptional and epigenetic factors (63, 66), and differential expression of microRNAs regulating Cx43 expression (67).

Using a fully humanized, spinal cord-specific, coculture platform to study ALS astrocyte/MN interactions, we were able to recapitulate previous studies (24, 27, 68–72) showing that ALS hiPSC-A were toxic to hiPSC-MN in coculture with FALS and SALS lines. Some variability in the degrees of neurotoxicity was noted among iPSC lines, which was expected and likely reflects the in vivo clinical, genetic, and pathogenic heterogeneity of ALS. Importantly, we could replicate this hiPSC-A toxicity neurotoxicity in two different MN lines. To identify specifically whether toxicity was mediated by the extracellular release of relevant toxic factors, we used a transwell system separating ALS hiPSC-A from hiPSC-MN. This system proved valuable as toxicity from ALS hiPSC-A was noted among all the lines. The differences in relative hiPSC-MN toxicity from ALS hiPSC-A between the coculture and transwell experiments could suggest that there are compensatory astrocyte-mediated neuroprotective factors manifested through the direct contact of astrocytes and MN, that may be eliminated in the transwell system. This direct contact could include spatial buffering of potassium, glutamate, and other metabolites away from synapses via an astrocytic GJ network at the level of the tripartite synapse (18, 73), the transport of glutamate via astrocytic perisynaptic glutamate transporters (74), stabilization of the synapse and perineuronal net by astrocyte released chondroitin sulfate proteoglycans (75), and the phagocytosis of dead neurons following injury as a mechanism of neuroprotection (76). The transwell cultures, and pharmacological blockade by the Gap19 mimetic peptide, show significant neuroprotection and implicate the release of factors through Cx43 HC into the media as a potent mediator of toxicity. This is further supported by our observation, not only that there are more Cx43 HC on the ALS hiPSC-A membrane, but they are functionally more active as well. We also noted, however, that blocking Cx43 HC was not sufficient to completely restore hiPSC-MN numbers to their control values. This supports previous work in the field suggesting that, in addition to Cx43 HC-mediated astrocyte toxicity, other mechanisms of ALS hiPSC-A induced MN toxicity are likely contributing as well.

To examine whether the cell-autonomous and Cx43-mediated astrocyte neurotoxicity is due to ALS mutations alone, we used a gene-correction strategy in the $SOD1^{A4V}$ mutation carrying hiPSC-A. Gene editing did not result in a complete rescue of astrocyte-mediated neurotoxicity, which paralleled the relatively higher expression of Cx43 retained in isogenic control cells compared to control lines. This may suggest that other factors, including epigenetic changes or as of yet unidentified risk-factor genes in both SALS and FALS, may represent ALS "disease signatures" contributing to residual astrocyte-mediated neurotoxicity, which are not affected by gene correction of FALS mutations (63). It is notable that the remaining neurotoxicity induced by isogenic $SOD1^{A4V}$ hiPSC-A was rescued by Gap19, suggesting that Cx43 HC contribute to this astrocyte-mediated phenomenon.

Several studies have suggested that astrocyte-mediated neurotoxicity in ALS appears to be specific to MN populations (23, 25, 26, 77). Our spinal cord-specific hiPSC platform of astrocyte/neuron cocultures may provide a more accurate window into spinal cord pathobiology. While the majority of our hiPSC-neurons are MN, (34), our data suggest that ALS hiPSC-A HC-mediated toxicity is not specific to MN subtypes but affects other neuronal subtypes and is consistent with ALS being increasingly recognized as a disorder not only of MN but GABAergic and glycinergic interneurons (78–80) as well.

One of the proposed strengths of using human iPSC is their potential use in translating fundamental observations to therapeutic opportunities (81). Mimetic peptides like Gap19 do not have the capacity to cross the blood brain barrier, and therefore their clinical use is limited. Tonabersat (SB-220453) (42) was selected for its specificity as a Cx43 HC blocker at low concentrations (42) as well as its ability to cross the blood brain barrier (48). Systemic delivery of tonabersat in low concentrations in a rat model of age-related macular degeneration improved functional outcomes by electroretinography and also prevented thinning of the retina through its capacity to block Cx43 HC (42). Tonabersat has been shown to reduce neurogenic inflammation, and antagonize transient neuronal hyperexcitability associated with cortical spreading depression in animal models of migraine with aura (82, 83), where a role of GJs has been proposed (84). Based upon this hypothesis and preclinical results, the oral administration of tonabersat was tested in a phase II clinical trial as a prophylaxis for migraine, where it was found to be well tolerated (85, 86). Tonabersat has also been tested on animal models of epilepsy (49, 50) and proposed as a novel antiepileptic therapy for clinical trials (87).

We therefore investigated the effect of tonabersat on MN survival and found that tonabersat displayed dose-dependent neuroprotective effects in the ALS hiPSC-A/MN coculture platform and, importantly, also in a transwell coculture model, consistent with its capacity to reduce Cx43 HC-mediated release of factors into the media. Interestingly, the neuroprotective effect of tonabersat was more robust in the direct coculture model when compared to the transwell coculture model. We hypothesize that this could reflect differences in Cx43 HC trafficking and localization to the astrocyte membrane or differences in Cx43 HC opening probability when astrocytes are separated from their MN counterparts, although these specific differences could not be definitively

identified. Since tonabersat has been shown to reduce astrocyte-mediated neuronal hyperexcitability, we used our recently established MEA recording technique (34) to test the effects of tonabersat on hiPSC-MN firing. We found that tonabersat reduces neuronal spiking and bursting activity in a dose-dependent fashion in control hiPSC-A/MN coculture. This effect was both astrocyte-specific, as the drug did not affect hiPSC-MN survival alone, and Cx43 HC-specific, as it occurred at concentrations of tonabersat known to specifically target HCs and was comparable to the electrophysiological effects of Gap19. We then translated this MEA platform for electrophysiological recording and drug testing to cultures of control and ALS hiPSC-A with control hiPSC-MN. The culture of human MN with ALS astrocytes resulted in a transient increase in neuronal firing early during the coculture period and, importantly, that this effect could be inhibited with acute addition of tonabersat. This study suggests, in an all-human iPSC model, that tonabersat can bring control MN firing rates back to normal in coculture with ALS astrocytes. Additional findings also support that treatment of ALS hiPSC-A/MN cocultures with tonabersat during a defined period of neuronal hyperexcitability was sufficient to provide long-lasting neuroprotection, suggesting that there is a temporal timeframe to the induction of astrocyte-mediated MN loss.

Having demonstrated, in our human iPSC in vitro platform, the efficacy of tonabersat in promoting MN neuroprotection, we examined some of its neuroprotective properties in vivo since this compound had not been previously administered chronically. Our data following chronic administration of tonabersat showed that Cx43 levels in $SOD1^{G93A}$ mice were unchanged, suggesting that any neuroprotective effect would not be related to loss of Cx43 but rather blocking of Cx43 HCs. The neuroprotective effect of tonabersat, while not evident during the early symptomatic phase, was observed at end stage as MNs were preserved in both cervical and lumbar spinal cords of $SOD1^{G93A}$ mice. This indicates that most of the neuroprotective effect of tonabersat occurred during the last 20 to 25 d leading up to end stage, and is reinforced by the observation that neuroprotection in the cervical spinal cord was also noted following tonabersat dosing beginning after the onset of disease, with treatment beginning at 100 d of age. This suggests, as seen with the $SOD1^{G93A}$:Cx43 KO mice, tonabersat does not alter the onset of disease but rather extends and confers preservation of MN during disease progression. Interestingly, while astrocyte Cx43 was unchanged following tonabersat treatment, GFAP expression (marker of reactive astrocytes) and Iba-1 (marker of microgliosis) were both reduced. Importantly, we did not see any detrimental effects on WT mice from tonabersat treatment beginning at 40 d of age. These observations suggest that tonabersat's in vitro neuroprotective effects are also translatable in the setting of chronic drug administration in vivo.

Using human ALS CNS tissue and CSF and showing increased expression of Cx43, as a potential biomarker of disease combined with the use of the human iPSC in vitro platform demonstrates the importance of Cx43 HC as contributors to ALS astrocyte-mediated neurotoxicity. The findings of this study offer potential for using Cx43 HC blockade for mediating ALS progression.

Methods

Cx43fl/fl:$SOD1^{G93A}$:GFAP-Cre Transgenic Mice. Transgenic $SOD1^{G93A}$:hGFAP-Cre: $Cx43^{fl/fl}$ mice were generated by breeding hGFAP-Cre on FVB background (Jackson Laboratories, JAX#004600) with $Cx43^{fl/fl}$ mice on C57BL6 background (Jackson Laboratories, JAX #008039), and those mice were further crossed with B6SJ/L $SOD1^{G93A}$ Gur/J mice (Jackson Laboratories, JAX #002726). Control littermates were used for all the experimental assays. All animal procedures were performed in accordance with the NIH guidelines on the care and use of vertebrate animals and approved by the Institutional Animal Care and Use Committee of the Research Institute at The Johns Hopkins University.

Human iPSC Astrocyte and hiPSC-MN Culture. The protocols for the use of human iPSC have undergone and received Johns Hopkins University Institutional Review Board approval. The titles of the protocols are "Skin biopsies and PBMCs generate cell lines for study of ALS" (approval 10/16/2008 NA_00021979) and "Generation and characterization of cell lines for ALS" (approval 1/19/2010 NA_00033726). Informed consent was obtained from all donors. Donations of samples were voluntary.

The generation, characterization of the human iPSC lines, and their differentiation into astrocytes have been previously described by our group and the lines utilized for this study are listed in *SI Appendix*, Table S2 (26, 34, 88). Human iPSC-A and hiPSC-MN coculture are described in *SI Appendix*.

MEA Culture and Recordings. MEA plates (MultiChannel Systems, 60MEA200/30iR-Ti-gr) with 60 electrodes, including 59 active and 1 reference, and an MEA2100 (MultiChannel Systems) platform were used for the recording of neuronal activity in hiPSC-A/-MN cocultures, as we have previously described (34).

Data Availability. All study data are included in the main text and *SI Appendix*.

ACKNOWLEDGMENTS. This study was supported in part by ALS Association 18-DDC-436 (to N.J.M.), Maryland Stem Cell Research Fund 2019-MSCRFD-5122 (to N.J.M.), The Packard Center for ALS research at The Johns Hopkins University (N.J.M.), Department of Defense ALSRP W81XWH1810175 (to N.J.M.), 1R01NS117604-01 (to N.J.M.), and NIH R01-GM099490 (to J.E.C.). The $SOD1^{A4V}$ isogenic lines were a kind gift from K.E. Amyotrophic lateral sclerosis and control brain and spinal cord tissues were obtained from the Target ALS Human Postmortem Tissue Core (Lyle Ostrow), as well as the VA Tissue Bank. Northeast ALS Consortium Sample Repository provided cerebrospinal fluid samples (James Berry). Illustrations were created with BioRender (https://biorender.com/).

1. U. Konietzko, C. M. Müller, Astrocytic dye coupling in rat hippocampus: Topography, developmental onset, and modulation by protein kinase C. *Hippocampus* **4**, 297–306 (1994).
2. A. Tabernero, C. Giaume, J. M. Medina, Endothelin-1 regulates glucose utilization in cultured astrocytes by controlling intercellular communication through gap junctions. *Glia* **16**, 187–195 (1996).
3. G. S. Goldberg, P. D. Lampe, B. J. Nicholson, Selective transfer of endogenous metabolites through gap junctions composed of different connexins. *Nat. Cell Biol.* **1**, 457–459 (1999).
4. Y. Qu, G. Dahl, Function of the voltage gate of gap junction channels: Selective exclusion of molecules. *Proc. Natl. Acad. Sci. U.S.A.* **99**, 697–702 (2002).
5. G. J. Christ, A. P. Moreno, A. Melman, D. C. Spray, Gap junction-mediated intercellular diffusion of Ca^{2+} in cultured human corporal smooth muscle cells. *Am. J. Physiol.* **263**, C373–C383 (1992).
6. T. S. Lawrence, W. H. Beers, N. B. Gilula, Transmission of hormonal stimulation by cell-to-cell communication. *Nature* **272**, 501–506 (1978).
7. J. C. Sáez, J. A. Connor, D. C. Spray, M. V. Bennett, Hepatocyte gap junctions are permeable to the second messenger, inositol 1,4,5-trisphosphate, and to calcium ions. *Proc. Natl. Acad. Sci. U.S.A.* **86**, 2708–2712 (1989).
8. L. Zong, Y. Zhu, R. Liang, H. B. Zhao, Gap junction mediated miRNA intercellular transfer and gene regulation: A novel mechanism for intercellular genetic communication. *Sci. Rep.* **6**, 19884 (2016).
9. L. S. Musil, D. A. Goodenough, Multisubunit assembly of an integral plasma membrane channel protein, gap junction connexin43, occurs after exit from the ER. *Cell* **74**, 1065–1077 (1993).
10. J. A. Orellana *et al.*, Modulation of brain hemichannels and gap junction channels by pro-inflammatory agents and their possible role in neurodegeneration. *Antioxid. Redox Signal.* **11**, 369–399 (2009).
11. L. Xing, T. Yang, S. Cui, G. Chen, Connexin hemichannels in astrocytes: Role in CNS disorders. *Front. Mol. Neurosci.* **12**, 23 (2019).
12. J. A. Orellana, Physiological functions of glial cell hemichannels. *Adv. Exp. Med. Biol.* **949**, 93–108 (2016).
13. R. Dermietzel, E. L. Hertberg, J. A. Kessler, D. C. Spray, Gap junctions between cultured astrocytes: Immunocytochemical, molecular, and electrophysiological analysis. *J. Neurosci.* **11**, 1421–1432 (1991).
14. J. E. Rash, T. Yasumura, F. E. Dudek, J. I. Nagy, Cell-specific expression of connexins and evidence of restricted gap junctional coupling between glial cells and between neurons. *J. Neurosci.* **21**, 1983–2000 (2001).
15. N. Rouach *et al.*, Gap junctions and connexin expression in the normal and pathological central nervous system. *Biol. Cell* **94**, 457–475 (2002).

16. C. Giaume, M. Theis, Pharmacological and genetic approaches to study connexin-mediated channels in glial cells of the central nervous system. *Brain Res. Brain Res. Rev.* **63**, 160–176 (2010).
17. A. Wallraff *et al.*, The impact of astrocytic gap junctional coupling on potassium buffering in the hippocampus. *J. Neurosci.* **26**, 5438–5447 (2006).
18. N. Rouach, A. Koulakoff, V. Abudara, K. Willecke, C. Giaume, Astroglial metabolic networks sustain hippocampal synaptic transmission. *Science* **322**, 1551–1555 (2008).
19. S. J. Mulligan, B. A. MacVicar, Calcium transients in astrocyte endfeet cause cerebrovascular constrictions. *Nature* **431**, 195–199 (2004).
20. A. M. Clement *et al.*, Wild-type nonneuronal cells extend survival of SOD1 mutant motor neurons in ALS mice. *Science* **302**, 113–117 (2003).
21. K. Yamanaka *et al.*, Astrocytes as determinants of disease progression in inherited amyotrophic lateral sclerosis. *Nat. Neurosci.* **11**, 251–253 (2008).
22. S. T. Papadeas, S. E. Kraig, C. O'Banion, A. C. Lepore, N. J. Maragakis, Astrocytes carrying the superoxide dismutase 1 (SOD1G93A) mutation induce wild-type motor neuron degeneration in vivo. *Proc. Natl. Acad. Sci. U.S.A.* **108**, 17803–17808 (2011).
23. M. Nagai *et al.*, Astrocytes expressing ALS-linked mutated SOD1 release factors selectively toxic to motor neurons. *Nat. Neurosci.* **10**, 615–622 (2007).
24. K. Qian *et al.*, Sporadic ALS astrocytes induce neuronal degeneration in vivo. *Stem Cell Reports* **8**, 843–855 (2017).
25. D. B. Re *et al.*, Necroptosis drives motor neuron death in models of both sporadic and familial ALS. *Neuron* **81**, 1001–1008 (2014).
26. A. M. Haidet-Phillips *et al.*, Astrocytes from familial and sporadic ALS patients are toxic to motor neurons. *Nat. Biotechnol.* **29**, 824–828 (2011).
27. K. Meyer *et al.*, Direct conversion of patient fibroblasts demonstrates non-cell autonomous toxicity of astrocytes to motor neurons in familial and sporadic ALS. *Proc. Natl. Acad. Sci. U.S.A.* **111**, 829–832 (2014).
28. S. A. Liddelow *et al.*, Neurotoxic reactive astrocytes are induced by activated microglia. *Nature* **541**, 481–487 (2017).
29. A. A. Almad *et al.*, Connexin 43 in astrocytes contributes to motor neuron toxicity in amyotrophic lateral sclerosis. *Glia* **64**, 1154–1169 (2016).
30. S. P. Yun *et al.*, Block of A1 astrocyte conversion by microglia is neuroprotective in models of Parkinson's disease. *Nat. Med.* **24**, 931–938 (2018).
31. M. A. Retamal, C. J. Cortés, L. Reuss, M. V. Bennett, J. C. Sáez, S-nitrosylation and permeation through connexin 43 hemichannels in astrocytes: Induction by oxidant stress and reversal by reducing agents. *Proc. Natl. Acad. Sci. U.S.A.* **103**, 4475–4480 (2006).
32. M. L. Ong, P. F. Tan, J. D. Holbrook, Predicting functional decline and survival in amyotrophic lateral sclerosis. *PLoS One* **12**, e0174925 (2017).
33. N. Atassi *et al.*, The PRO-ACT database: Design, initial analyses, and predictive features. *Neurology* **83**, 1719–1725 (2014).
34. A. Taga *et al.*, Role of human-induced pluripotent stem cell-derived spinal cord astrocytes in the functional maturation of motor neurons in a multielectrode array system. *Stem Cells Transl. Med.* **8**, 1272–1285 (2019).
35. W. J. Broom *et al.*, Variants in candidate ALS modifier genes linked to Cu/Zn superoxide dismutase do not explain divergent survival phenotypes. *Neurosci. Lett.* **392**, 52–57 (2006).
36. J. A. Orellana *et al.*, ATP and glutamate released via astroglial connexin 43 hemichannels mediate neuronal death through activation of pannexin 1 hemichannels. *J. Neurochem.* **118**, 826–840 (2011).
37. V. Abudara *et al.*, The connexin43 mimetic peptide Gap19 inhibits hemichannels without altering gap junctional communication in astrocytes. *Front. Cell. Neurosci.* **8**, 306 (2014).
38. A. Chiò *et al.*, The role of APOE in the occurrence of frontotemporal dementia in amyotrophic lateral sclerosis. *JAMA Neurol.* **73**, 425–430 (2016).
39. S. Kato *et al.*, Absence of SOD1 gene abnormalities in familial amyotrophic lateral sclerosis with posterior column involvement without Lewy-body-like hyaline inclusions. *Acta Neuropathol.* **92**, 528–533 (1996).
40. Y. S. Guo *et al.*, Sensory involvement in the SOD1-G93A mouse model of amyotrophic lateral sclerosis. *Exp. Mol. Med.* **41**, 140–150 (2009).
41. E. Kiskinis *et al.*, Pathways disrupted in human ALS motor neurons identified through genetic correction of mutant SOD1. *Cell Stem Cell* **14**, 781–795 (2014).
42. Y. Kim *et al.*, Tonabersat prevents inflammatory damage in the central nervous system by blocking connexin43 hemichannels. *Neurotherapeutics* **14**, 1148–1165 (2017).
43. Q. Chen *et al.*, Carcinoma-astrocyte gap junctions promote brain metastasis by cGAMP transfer. *Nature* **533**, 493–498 (2016).
44. P. S. Gaete, J. E. Contreras, A method for assessing ionic and molecular permeation in connexin hemichannels. *Methods Enzymol.* **654**, 271–293 (2021).
45. W. N. Chan *et al.*, Identification of (-)-cis-6-acetyl-4S-(3-chloro-4-fluoro-benzoylamino)- 3,4-dihydro-2,2-dimethyl-2H-benzo[b]pyran-3S-ol as a potential antimigraine agent. *Bioorg. Med. Chem. Lett.* **9**, 285–290 (1999).
46. H. J. Herdon *et al.*, Characterization of the binding of [3H]-SB-204269, a radiolabelled form of the new anticonvulsant SB-204269, to a novel binding site in rat brain membranes. *Br. J. Pharmacol.* **121**, 1687–1691 (1997).
47. J. F. Tvedskov, H. K. Iversen, J. Olesen, A double-blind study of SB-220453 (Tonerbasat) in the glyceryltrinitrate (GTN) model of migraine. *Cephalalgia* **24**, 875–882 (2004).
48. D. P. Bradley *et al.*, Diffusion-weighted MRI used to detect in vivo modulation of cortical spreading depression: Comparison of sumatriptan and tonabersat. *Exp. Neurol.* **172**, 342–353 (2001).
49. N. Upton *et al.*, Profile of SB-204269, a mechanistically novel anticonvulsant drug, in rat models of focal and generalized epileptic seizures. *Br. J. Pharmacol.* **121**, 1679–1686 (1997).
50. N. Upton, M. Thompson, Benzo[b]pyranols and related novel antiepileptic agents. *Prog. Med. Chem.* **37**, 177–200 (2000).
51. J. E. Rash *et al.*, Identification of cells expressing Cx43, Cx30, Cx26, Cx32 and Cx36 in gap junctions of rat brain and spinal cord. *Cell Commun. Adhes.* **8**, 315–320 (2001).
52. R. Ren, L. Zhang, M. Wang, Specific deletion connexin43 in astrocyte ameliorates cognitive dysfunction in APP/PS1 mice. *Life Sci.* **208**, 175–191 (2018).
53. C. Yi *et al.*, Astroglial connexin43 contributes to neuronal suffering in a mouse model of Alzheimer's disease. *Cell Death Differ.* **23**, 1691–1701 (2016).
54. C. Yi *et al.*, Inhibition of glial hemichannels by boldine treatment reduces neuronal suffering in a murine model of Alzheimer's disease. *Glia* **65**, 1607–1625 (2017).
55. Y. Wang, Z. Wu, X. Liu, Q. Fu, Gastrodin ameliorates Parkinson's disease by downregulating connexin 43. *Mol. Med. Rep.* **8**, 585–590 (2013).
56. M. Freitas-Andrade, C. C. Naus, Astrocytes in neuroprotection and neurodegeneration: The role of connexin43 and pannexin1. *Neuroscience* **323**, 207–221 (2016).
57. P. Díaz-Amarilla *et al.*, Phenotypically aberrant astrocytes that promote motoneuron damage in a model of inherited amyotrophic lateral sclerosis. *Proc. Natl. Acad. Sci. U.S.A.* **108**, 18126–18131 (2011).
58. A. F. Keller, M. Gravel, J. Kriz, Treatment with minocycline after disease onset alters astrocyte reactivity and increases microgliosis in SOD1 mutant mice. *Exp. Neurol.* **228**, 69–79 (2011).
59. Y. Cui *et al.*, Extensive dysregulations of oligodendrocytic and astrocytic connexins are associated with disease progression in an amyotrophic lateral sclerosis mouse model. *J. Neuroinflammation* **11**, 42 (2014).
60. C. Huang *et al.*, Critical role of connexin 43 in secondary expansion of traumatic spinal cord injury. *J. Neurosci.* **32**, 3333–3338 (2012).
61. O. Peters *et al.*, Astrocyte function is modified by Alzheimer's disease-like pathology in aged mice. *J. Alzheimers Dis.* **18**, 177–189 (2009).
62. J. I. Nagy, W. Li, E. L. Hertzberg, C. A. Marotta, Elevated connexin43 immunoreactivity at sites of amyloid plaques in Alzheimer's disease. *Brain Res.* **717**, 173–178 (1996).
63. K. Kim *et al.*, Epigenetic memory in induced pluripotent stem cells. *Nature* **467**, 285–290 (2010).
64. A. Almad, N. J. Maragakis, A stocked toolbox for understanding the role of astrocytes in disease. *Nat. Rev. Neurol.* **14**, 351–362 (2018).
65. C. D'hondt *et al.*, Nutrient starvation decreases Cx43 levels and limits intercellular communication in primary bovine corneal endothelial cells. *J. Membr. Biol.* **249**, 363–373 (2016).
66. M. Oyamada, K. Takebe, Y. Oyamada, Regulation of connexin expression by transcription factors and epigenetic mechanisms. *Biochim. Biophys. Acta* **1828**, 118–133 (2013).
67. Y. Lei, X. Peng, T. Li, L. Liu, G. Yang, ERK and miRNA-1 target Cx43 expression and phosphorylation to modulate the vascular protective effect of angiotensin II. *Life Sci.* **216**, 59–66 (2019).
68. M. Madill *et al.*, Amyotrophic lateral sclerosis patient iPSC-derived astrocytes impair autophagy via non-cell autonomous mechanisms. *Mol. Brain* **10**, 22 (2017).
69. F. P. Di Giorgio, M. A. Carrasco, M. C. Siao, T. Maniatis, K. Eggan, Non-cell autonomous effect of glia on motor neurons in an embryonic stem cell-based ALS model. *Nat. Neurosci.* **10**, 608–614 (2007).
70. S. P. Allen *et al.*, Astrocyte adenosine deaminase loss increases motor neuron toxicity in amyotrophic lateral sclerosis. *Brain* **142**, 586–605 (2019).
71. C. E. Hall *et al.*, Progressive motor neuron pathology and the role of astrocytes in a human stem cell model of VCP-related ALS. *Cell Rep.* **19**, 1739–1749 (2017).
72. A. Birger *et al.*, Human iPSC-derived astrocytes from ALS patients with mutated C9ORF72 show increased oxidative stress and neurotoxicity. *EBioMedicine* **50**, 274–289 (2019).
73. A. Verkhratsky, R. Zorec, Astroglial signalling in health and disease. *Neurosci. Lett.* **689**, 1–4 (2019).
74. K. P. Lehre, L. M. Levy, O. P. Ottersen, J. Storm-Mathisen, N. C. Danbolt, Differential expression of two glial glutamate transporters in the rat brain: Quantitative and immunocytochemical observations. *J. Neurosci.* **15**, 1835–1853 (1995).
75. N. A. Perez-Catalan, C. Q. Doe, S. D. Ackerman, The role of astrocyte-mediated plasticity in neural circuit development and function. *Neural Dev.* **16**, 1 (2021).
76. C. Löövy, L. Hillered, T. Ebendal, A. Erlandsson, Engulfing astrocytes protect neurons from contact-induced apoptosis following injury. *PLoS One* **7**, e33090 (2012).
77. S. Song *et al.*, Major histocompatibility complex class I molecules protect motor neurons from astrocyte-induced toxicity in amyotrophic lateral sclerosis. *Nat. Med.* **22**, 397–403 (2016).
78. B. M. Morrison, J. W. Gordon, M. E. Ripps, J. H. Morrison, Quantitative immunocytochemical analysis of the spinal cord in G86R superoxide dismutase transgenic mice: Neurochemical correlates of selective vulnerability. *J. Comp. Neurol.* **373**, 619–631 (1996).
79. H. Tsuiji *et al.*, TDP-43 accelerates age-dependent degeneration of interneurons. *Sci. Rep.* **7**, 14972 (2017).
80. M. Hossaini *et al.*, Spinal inhibitory interneuron pathology follows motor neuron degeneration independent of glial mutant superoxide dismutase 1 expression in SOD1-ALS mice. *J. Neuropathol. Exp. Neurol.* **70**, 662–677 (2011).
81. J. P. Richard, N. J. Maragakis, Induced pluripotent stem cells from ALS patients for disease modeling. *Brain Res.* **1607**, 15–25 (2015).
82. P. L. Durham, F. G. Garrett, Neurological mechanisms of migraine: Potential of the gap-junction modulator tonabersat in prevention of migraine. *Cephalalgia* **29** (suppl. 2), 1–6 (2009).
83. S. Damodaram, S. Thalakoti, S. E. Freeman, F. G. Garrett, P. L. Durham, Tonabersat inhibits trigeminal ganglion neuronal-satellite glial cell signaling. *Headache* **49**, 5–20 (2009).
84. D. Sarrouilhe, C. Dejean, M. Mesnil, Involvement of gap junction channels in the pathophysiology of migraine with aura. *Front. Physiol.* **5**, 78 (2014).
85. A. W. Hauge, M. S. Asghar, H. W. Schytz, K. Christensen, J. Olesen, Effects of tonabersat on migraine with aura: A randomised, double-blind, placebo-controlled crossover study. *Lancet Neurol.* **8**, 718–723 (2009).
86. P. J. Goadsby, M. D. Ferrari, A. Csanyi, J. Olesen, J. G. Mills; Tonabersat TON-01-05 Study Group, Randomized, double-blind, placebo-controlled, proof-of-concept study of the cortical spreading depression inhibiting agent tonabersat in migraine prophylaxis. *Cephalalgia* **29**, 742–750 (2009).
87. M. Bialer *et al.*, Progress report on new antiepileptic drugs: A summary of the Eleventh Eilat Conference (EILAT XI). *Epilepsy Res.* **103**, 2–30 (2013).
88. L. Roybon *et al.*, Human stem cell-derived spinal cord astrocytes with defined mature or reactive phenotypes. *Cell Rep.* **4**, 1035–1048 (2013).